PLOS ONE

RESEARCH ARTICLE

Impact of Maxwell velocity slip and Smoluchowski temperature slip on CNTs with modified Fourier theory: Reiner-Philippoff model

Tanveer Sajid[1], Wasim Jamshed[1], Faisal Shahzad[1], M. A. Aiyashi[2], Mohamed R. Eid[3,4]*, Kottakkaran Sooppy Nisar[5], Anurag Shukla[6]

1 Department of Mathematics, Capital University of Science and Technology (CUST), Islamabad, Pakistan, **2** Department of Mathematics, College of Science, Jazan University, Jazan, Saudi Arabia, **3** Department of Mathematics, Faculty of Science, New Valley University, Al-Kharga, Al-Wadi Al-Gadid, Egypt, **4** Department of Mathematics, Faculty of Science, Northern Border University, Arar, Saudi Arabia, **5** Department of Mathematics, College of Arts and Sciences, Prince Sattam bin Abdulaziz University, Wadi Aldawaser, Saudi Arabia, **6** Department of Applied Science, Rajkiya Engineering College Kannauj, Kannauj, India

* m_r_eid@yahoo.com

Citation: Sajid T, Jamshed W, Shahzad F, Aiyashi MA, Eid MR, Nisar KS, et al. (2021) Impact of Maxwell velocity slip and Smoluchowski temperature slip on CNTs with modified Fourier theory: Reiner-Philippoff model. PLoS ONE 16(10): e0258367. https://doi.org/10.1371/journal.pone.0258367

Editor: Mohammad Mehdi Rashidi, Tongji University, CHINA

Received: June 4, 2021

Accepted: September 25, 2021

Published: October 14, 2021

Data Availability Statement: All relevant data are within the manuscript.

Funding: No financial support for the research, authorship, and publication of this article was obtained by the authors.

Competing interests: The authors have declared that no competing interests exist.

Abstract

The present article presents a novel idea regarding the implementation of Tiwari and Das model on Reiner-Philippoff fluid (RPF) model by considering blood as a base fluid. The Cattaneo-Christov model and thermal radiative flow have been employed to study heat transfer analysis. Tiwari and Das model consider nanoparticles volume fraction for heat transfer enhancement instead of the Buongiorno model which heavily relies on thermophoresis and Brownian diffusion effects for heat transfer analysis. Maxwell velocity and Temperature slip boundary conditions have been employed at the surface of the sheet. By utilizing the suitable transformations, the modeled PDEs (partial-differential equations) are renewed in ODEs (ordinary-differential equations) and treated these equations numerically with the aid of bvp4c technique in MATLAB software. To check the reliability of the proposed scheme a comparison with available literature has been made. Other than Buongiorno nanofluid model no attempt has been made in literature to study the impact of nanoparticles on Reiner-Philippoff fluid model past a stretchable surface. This article fills this gap available in the existing literature by considering novel ideas like the implementation of carbon nanotubes, CCHF, and thermal radiation effects on Reiner-Philippoff fluid past a slippery expandable sheet. Momentum, as well as temperature slip boundary conditions, are never studied and considered before for the case of Reiner-Philippoff fluid past a slippery expandable sheet. In the light of physical effects used in this model, it is observed that heat transfer rate escalates as a result of magnification in thermal radiation parameter which is 18.5% and skin friction coefficient diminishes by the virtue of amplification in the velocity slip parameter and maximum decrement is 67.9%.

1. Introduction

Since 1991, this is the subject of the inquiry because of its synthetic and basic existence since the beginnings of the era of carbon nanotubes. In several technical and industrial applications such as electrochemical super-capacitors, transistors, sensors and field emitting machines, engine transmission oil, heat exhaust flue gas recovery, electrical cooling, nuclear cooling, nanofluid boiling, etc. special properties such as high surface radiation, carbon nanotubes (CNTs) were studied. These applications got the researcher's attention to work on CNTs. Kundu et al. [1] presented a carbon nanotube-based superior convective flow of Maxwell nanoliquid over an expanding sheet embedded through multiple slip influences. Al-Hanaya et al. [2] inspected the impact of single and multiwall carbon nanotubes on micropolar fluid along an extendable surface. Hayat et al. [3] published a computational approach on diffusion-species of carbon nanotubes. Nagalakshm et al. [4] pondered the magnetohydrodynamic (MHD) radiative flow of an incompressible steady flow of Carreau nanofluid along with carbon nanotubes affecting through a nonlinear elongated plate. Muhammad et al. [5] established the mathematical scheme concerning a Casson fluid through a stretching surface along in existence of CNTs, thermal non-linear radiation, and heat sink (source). Khalid et al. [6] pondered the impression of MHD and CNTs on fluid movement through an expandable plate. Hosseinzadeh et al. [7, 8] investigated cross-fluid flow past a cylinder and rotate cone with the inclusion of nanoparticles and motile gyrotactic microorganisms. Lu et al. [9] analyzed the behaviour of nanoliquids containing CNTs along with a CCHF and entropy production. The impact of carbon nanotubes on mixed convective radiative liquid flowing past a nonlinearly elongated sheet along with slip constraint is inspected by Mandal et al. [10]. Chaudhary et al. [11] elaborated the viscous nanofluid flowing with electrical conductivity close to a stagnating area of CNTs in water via extending surface. Researchers have employed the law of conduction suggested by Fourier to evaluate the heat transport analysis of liquid. Research investigations [12–15] probed the impacts of CNTs, MoS_2, and Fe_3O_4 hybrid nanoparticles with the consideration of different base fluids moving over diverse surfaces. Cattaneo [16] modified the Fourier law of conduction by inserting the relaxation time phenomenon for the heat-flux and later on Christov [17] introduced a derivative prototypical of Cattaneo's rule and that developed known as Cattaneo-Christov law having immense applications in the engineering and medical field like nuclear reactor cooling, pasteurization of milk, electronic devices, hybrid power generators, etc. Based on these applications Akbar et al. [18] discussed the magnetic field and CCHF effects on CNTs-water nanofluid moving via an expandable plate. Ali et al. [19] pondered the characteristics of Cattaneo-Christov diffusion model for the flow of stagnancy point of Carreau nanofluid along an extendable surface embedded with chemical reaction effect. Ibrahim et al. [20] checked the flux impact of Cattaneo-Christov on free convective incompressible viscous fluid flowing through a vertical plate along with viscous dissipation and thermal radiation. Rasool et al. [21] researched to disclose the features of the inhomogeneous induced magnetical impact of nanoliquid flowing manifested with CCHF effect via an exponential extendable sheet. Khan et al. [22] scrutinized the impact of three different types of nanoparticles like Al_2O_3, TiO_2 and copper Cu by considering H_2O as a standard liquid through a nonlinearly expandable plate embedded with the CCHF. Shah et al. [23] investigated the effect of carbon nanotubes and CCHF on three-dimensional rotating liquid past an extendable plate. In the thermal radiation incidence model of the Cattaneo-Christov system, Dogonchi et al. [24] studied the heat transport analyzes of nanofluid flow between two parallel plating model.

Thermal radiation is one of three processes that permit energy exchange for bodies with different temperatures. The electro-magnetic wave emission from substances is characterized by

thermal radiation (variation of its interior energy). It transmits radiation from ultraviolet to far-field infrasound depending on the material's temperature. Thermal radioactivity is utilized where the high-temperature variance is essential having immense utilization in the industry like thermal furnaces, nuclear reactors, polymer production, combustion reactors, rubber production, etc. Sreedevi and Reddy [25] pondered the impact of thermal radiation on multi-wall carbon nanotube with kerosene as a base fluid past an extendable surface and found that the temperature field escalates owing to an increment in the thermal radiation parameter. The thin-film stream of a viscous nanofluid is introduced by Shah et al. [26] over a horizontal, spinning disk immersed in thermal radiative effect. Reddy et al. [27] inspected the influence of thermal radiative flow and viscous dissipative on RPF via a porous medium. Khan et al. [28] probed the impacts of thermophoretic and thermal radiative flow on second-grade two-dimensional magneto-liquid in which viscous dissipative is introduced via a stretchable surface. Hosseinzadeh et al. [29] scrutinized the influence of thermal radiation and viscous dissipation on hybrid nanoparticles over the vertical cylinder with the consideration of different shapes of nanoparticles. Kumar et al. [30] explored the effect of viscous dissipative and Joule effect on 3-dimensional nanofluid flow of Jeffrey model past an extending sheet underneath the influence of thermal exponential radiation. Makinde et al. [31] deliberated the influence of thermal radiative and melting heat transfer on magneto micropolarity liquid through an elongated sheet. The influence of thermal radiative flow and viscous dissipative on water squeezing among two Riga surfaces is scrutinized by Ahmed et al. [32]. The impact of nanoparticles, microorganisms, and thermal radiation on bioconvection past a magnetic field has been debated in detail by Hosseinzadeh et al. [33]. Hybrid nanoparticles fluid flow through an octagonal porous medium with the inclusion of MHD and thermal radiation are scrutinized by Hosseinzadeh et al. [34]. Rashed et al. [35] observed the effect of thermal radiative flow and magnetohydrodynamics over a porous rotating infinite disk together with Soret and Dufour effects.

The slip-free effect happens where the fluid and the wall are equal in velocity. On the other hand, the state in which the fluid and the wall velocity are different is called the slip velocity. In the case of temperature slip of the fluid and the sheet surface temperature is different. The liquid impact of boundary slip has distinguished utilizations like improving artificial interior cavities and valves of the heart. Shafiq et al. [36], under the simultaneous influence of thermal slip and the convective boundary conditions, examined revolving frame fluid flow. In presence of slip boundary conditions, Mukhopadhyay [37] conducted a thorough analysis of the unstable convective boundary layer flow and the heat transfer over the vertical stretch field. Thanks to the increase of the speed slip parameter the rate of heat transfer decreases. For the thermal slip parameter, the same function is noted also. Raza et al. [38] investigated thermal radiation and slip velocity effects concurrently with a heated convective stretching plate. Abbas et al. [39] exhibited the flow of hybrid nanoparticles with slip velocity and MHD. In the presence of thermal and hydrodynamic slip conditions, Rao et al. [40] proposed the laminar free convective boundary-layer flow of a Casson viscoelastic fluid external to a vertical permeable spherical cone. The results of the thermal and velocity boundary conditions on thermally radiative ferrofluid motions over a flat plate are studied by Sejunit and Khaleque [41]. Li and Keh [42] discussed analytically the thermophoretic displacement of the spherical particles at the core of a gaseous material in the specified temperature gradient. Sarabandi and Moghadam [43] analyzed the steady-state laminar flow of non-Newtonian fluid in a circular microchannel embedded with slip velocity condition.

The reasons behind the organization of this research are given below:

- The Maxwell velocity and Smoluchowski temperature boundary slip constraints are considered to study a slip effect on RPF which is not explored yet in available literature. Before

this investigation, no literature is available to study the effect of Maxwell velocity and Smoluchowski temperature jump boundary conditions on the Non-newtonian fluid past a stretching sheet.

- Other than Buongiorno nanofluid no literature is available to study the effect of nanoparticles on Reiner-Philippoff fluid past a stretching sheet. Attempt has been made in this article to implement Tiwari and Das nanofluid model for the case of heat transport analysis of Reiner-Philippoff model with blood as a standard fluid.
- Before this investigation, no literature on Reiner-Philippoff fluid is available to study heat flux of Cattaneo-Christov scheme along with thermal radiation is used to investigate the heat transfer analysis. Thermal radiation present in the fluid amplifies the heat transfer rate. The main purpose is to investigate the heat transfer rate with the inclusion of CCHF and thermal radiation.
- SWCNT/MWCNT are never used before for the case of Riner-Philippoff fluid.

2. Flow model

The expression Reiner-Philippoff [27] of stress deformation is given:

$$\frac{\partial u}{\partial y} = \frac{\tau}{\mu_\infty + \frac{\mu_0 - \mu_\infty}{1+\left(\frac{\tau}{\tau_s}\right)^2}}. \tag{1}$$

The symbols τ, τ_s, μ_0 and μ_∞ indicates shear-stress, reference shear-stress, zero shear viscosity, and limited viscosity. Reiner-Philippoff model responds like shear thinning, Newtonian, and shear thickening subjected to a variation in fluid viscosity. Mathematical expression regarding RPF flow function is written as

$$f(\sigma) = \frac{\sigma}{1 + \frac{\lambda - 1}{1+\sigma^2}}, \tag{2}$$

whereas $\sigma = \frac{\tau}{\tau_s}$ and $\lambda = \frac{\mu_0}{\mu_\infty}$. The expression λ in fluid flow function represents Reiner-Philippoff fluid parameter. Reiner-Philippoff behaviour is Newtonian for $\lambda = 1$, shear thickening $\lambda<0$, and shear thinning $\lambda>1$.

Fig 1 is designed to reflect the physical interpretation of RPF impinging on an expanding surface having an extending velocity u_w influential lengthways x–direction. The symbols T_0 and T_∞ depicts the fluid energy and concentration at the surface and ambient temperature outlying from the surface. The momentum equation has been scrutinized with the inclusion of carbon nanotubes. Momentum and thermal boundary layers occur when the velocity and temperature of the fluid is 0.99% of the free stream fluid velocity as well as temperature. Under these boundary conditions, the viscous, as well as velocity effects, hold. Heat transfer analysis has been carried out with the inclusion of solar thermal thermal and CCHF. Radiation is one of the best sources of heat and requires no medium for its propagation. Heat transfer rate in the case of the temperature equation is improved with the inclusion of carbon nanotubes, CCHF, and thermal radiation. Momentum and temperature slip boundary conditions have been employed at the boundary surface by the consideration of the assumption that the surface is rough, wet, and the effect of the adhesive forces is negligible. The fluid is incompressible and laminar. The density, as well as pressre, is constant. Human blood is considered as a base liquid flowing through a stretchable surface with the inclusion of SWCNT and MWCNT. The density ρ_{nf}, thermal diffusion α_{nf}, nanofluid specific heat $(\rho C_p)_{nf}$, thermal conductance k_{nf} are specified by the mathematical expressions mentioned below [1–3]. Fig 2 demonstrates the flow chart of

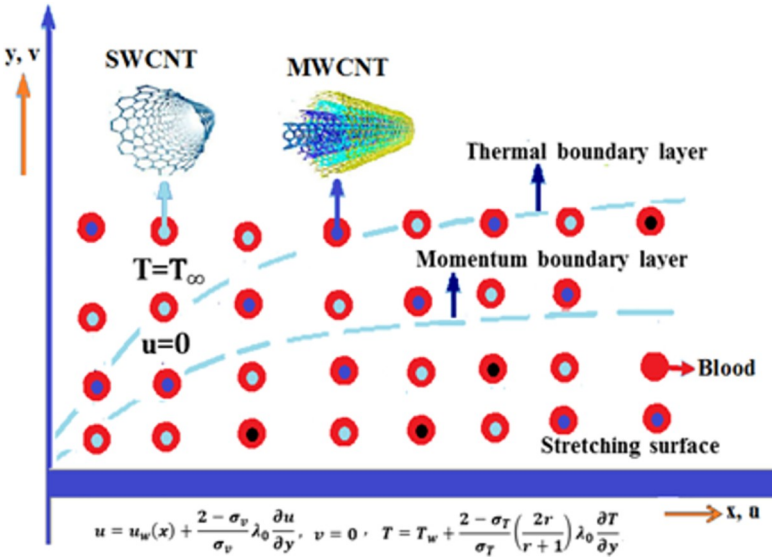

Fig 1. Physical description of flow model.

https://doi.org/10.1371/journal.pone.0258367.g001

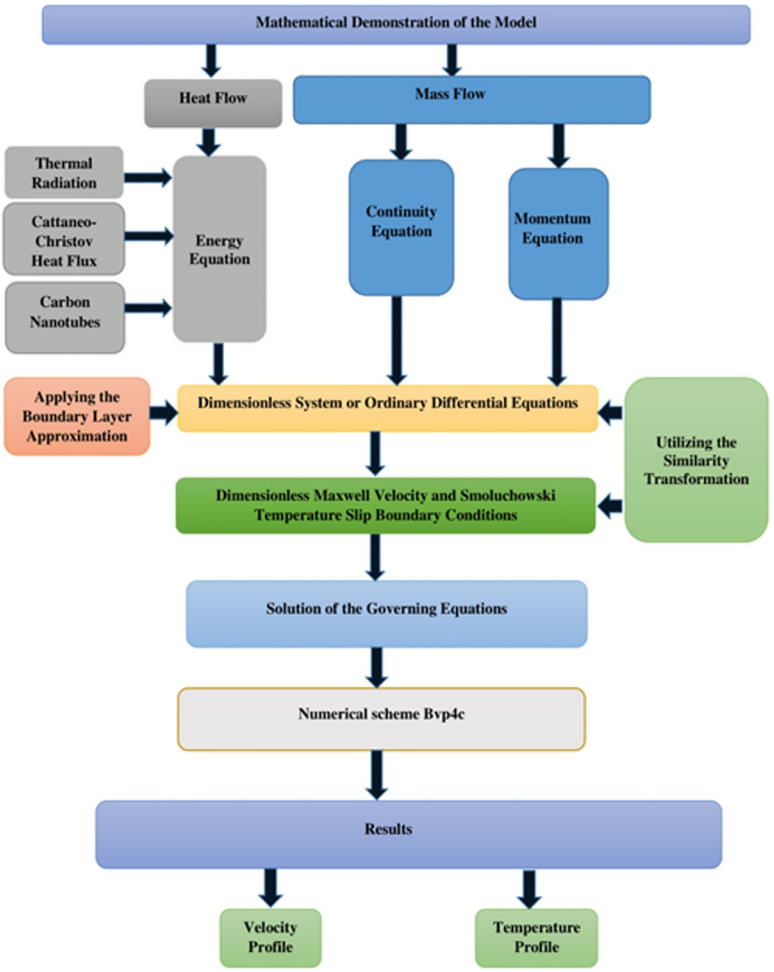

Fig 2. Mathematical model's flow chart structure.

https://doi.org/10.1371/journal.pone.0258367.g002

a mathematical model.

$$\left.\begin{aligned}
&\rho_{nf} = (1-\phi)\rho_f + \phi\rho_{CNT},\\
&\mu_{nf} = \frac{\mu_f}{1-\phi_{2.5}},\\
&\alpha_{nf} = \frac{k_{nf}}{(\rho C_p)_{nf}},\\
&(\rho C_p)_{nf} = (1-\phi)(\rho C_p)_f + \phi(\rho C_p)_{CNT},\\
&\frac{k_{nf}}{k_f} = \frac{(1-\phi) + 2\phi\frac{k_{CNT}}{k_{CNT}-k_f} ln\frac{k_{CNT}+k_f}{2k_f}}{(1-\phi) + 2\phi\frac{k_f}{k_{CNT}-k_f} ln\frac{k_{CNT}+k_f}{2k_f}},
\end{aligned}\right\} \tag{3}$$

Table 1 displays the thermo-physical features of essential fluid and CNTs below [6].
The models of the continuity, momentum, and energy equations are described below [27]:

$$\frac{\partial u}{\partial x} + \frac{\partial v}{\partial y} = 0, \tag{4}$$

$$u\frac{\partial u}{\partial x} + v\frac{\partial u}{\partial y} = \nu_{nf}\frac{\partial \tau}{\partial y}, \tag{5}$$

$$u\frac{\partial T}{\partial x} + v\frac{\partial T}{\partial y} + \lambda_E\Phi_E = \frac{k_{nf}}{(\rho C_p)_{nf}}\frac{\partial^2 T}{\partial y^2} - \frac{1}{(\rho C_p)_{nf}}\frac{\partial q_r}{\partial y}, \tag{6}$$

The physical boundary conditions (BCs) are [27]:

$$\left.\begin{aligned}
&y = 0 : u(x,y) = ax^{\frac{1}{3}} + \frac{2-\sigma_v}{\sigma_v}\lambda_0 x^{\frac{1}{3}}\frac{\partial u}{\partial y}, v = 0, T = T_0 + \frac{2-\sigma_T}{\sigma_T}\left(\frac{2r}{r+1}\right)\frac{\lambda_0}{Pr}x^{\frac{1}{3}}\frac{\partial T}{\partial y}\\
&y \to \infty : u \to 0, T \to T_\infty,
\end{aligned}\right\} \tag{7}$$

where CCHF [19–22] is given by

$$\Phi_E = \left(u^2\frac{\partial^2 T}{\partial x^2} + v^2\frac{\partial^2 T}{\partial y^2} + 2uv\frac{\partial^2 T}{\partial x \partial y}\right) + \left(\left(u\frac{\partial u}{\partial x} + v\frac{\partial u}{\partial y}\right)\frac{\partial T}{\partial x} + \left(u\frac{\partial v}{\partial x} + v\frac{\partial v}{\partial y}\right)\frac{\partial T}{\partial y}\right). \tag{8}$$

The expression of heat radiation flux [32] is specified as

$$q_r = -\frac{4\sigma^*}{3\kappa^*}\frac{\partial T^4}{\partial y} = -\frac{16\sigma^*}{3\kappa^*}T^3\frac{\partial T}{\partial y}. \tag{9}$$

Table 1. Thermo-physical characteristics.

Property	Human Blood (38˚C)	SWCNT	MWCNT
C_p	3594	425	796
ρ	1053	2600	1600
k	0.492	6600	3000
Pr	24	-	-

https://doi.org/10.1371/journal.pone.0258367.t001

The function of a stream is defined as $u = \frac{\partial \psi}{\partial y}$ and $v = \frac{-\partial \psi}{\partial x}$. By utilizing the appropriate similarity transformation [27] with velocity $U(x) = ax^{\frac{1}{3}}$ given below

$$\left.\psi = \sqrt{av}x^{\frac{2}{3}}f(\eta), \eta = \sqrt{\frac{a}{v}}x^{\frac{-1}{3}}y, \tau = \rho\sqrt{a^3v}g(\eta), \theta(\eta) = \frac{T - T_\infty}{T_0 - T_\infty},\right\} \tag{10}$$

the Eqs (4)–(6) are transformed into non-dimensionless ODEs

$$g' = \frac{A_1}{3}f'^2 - \frac{2}{3}ff'', \tag{11}$$

$$g = f''\frac{\gamma^2 + \lambda\gamma^2}{\gamma^2 + \gamma^2}, \tag{12}$$

$$\left(A_2 + \frac{4}{3}Rd\right)\theta'' + \frac{2}{3}{}_3\Pi\rho\phi\theta' - \Pi\rho\delta(\phi\phi'\theta' + \eta\phi^2\theta'') = 0, \tag{13}$$

associated boundary conditions are

$$\left.\begin{aligned}&\eta = 0 : f(\eta) = 0, f'(\eta) = 1 + \gamma_1 f'', \theta(\eta) = 1 + \gamma_2\theta',\\ &\eta \to \infty : f'(\eta) \to 0, \theta(\eta) \to 0.\end{aligned}\right\} \tag{14}$$

The associated non-dimensionless quantities are defined below

$$\left.\begin{aligned}&\gamma = \left(\frac{\tau_s}{\rho\sqrt{a^3v}}\right), \lambda = \frac{\mu_0}{\mu_\infty}, Pr = \frac{\mu C_p}{k_\infty}, R_d = \frac{16\sigma T_\infty^3}{3k^* k_\infty}, \delta = a\lambda_E\\ &\gamma_1 = \frac{2 - \sigma_v}{\sigma_v}\lambda_0\sqrt{\frac{a}{v}}, \gamma_2 = \frac{2 - \sigma_T}{\sigma_T}\left(\frac{2r}{r+1}\right)\frac{\lambda_0}{Pr}\sqrt{\frac{a}{v}},\end{aligned}\right\} \tag{15}$$

where A_1, A_2 and A_3 are given by

$$\left.\begin{aligned}A_1 &= \frac{1}{(1-\phi) + \phi\frac{\rho_{CNT}}{\rho_f}},\\ A_2 &= \frac{k_{nf}}{k_f},\\ A_3 &= (1-\phi) + \phi\frac{(\rho C_p)_{CNT}}{(\rho C_p)_f}.\end{aligned}\right\} \tag{16}$$

3. Physical quantities

The mathematical expression regarding skin friction coefficient [27] is given by

$$Cf_x = \frac{\tau}{\frac{U_w^2}{2}}, \tag{17}$$

after utilizing the similarity transformation the non-dimensionless formula of drag force coefficient is

$$\frac{1}{2}Cf_x Re_x^{1/2} = g(0). \tag{18}$$

The expression regarding heat transfer Nusselt number [27] is

$$Nu_x = \frac{xq_w}{k_f(T_0 - T_\infty)}, \tag{19}$$

whereas q_w indicates heat flux having expression mentioned below

$$q_w = -k_{nf}\left(\frac{\partial T}{\partial y}\right)_{y=0} + q_r. \tag{20}$$

The dimensionless Nusselt number after utilization of similarity transformation is manifested by

$$Nu_x Re_x^{-1/2} = -A_2\theta'(0), \tag{21}$$

4. Solution methodology

The MATLAB bvp4c which is the finite-difference scheme (collocation scheme) is executed to evaluate the non-dimensionless system of Eqs (12)–(14) sideways with boundary constraints (15). After allocating $f = w_1, f' = w_2, f'' = w_3, \theta = w_4$, the system of ODEs are converted into first order, represented by

$$\left.\begin{aligned} w_1' &= w_2, \\ w_2' &= \frac{w_3 w_3^2 + \gamma^2}{w_3^2 + \lambda\gamma^2}, \\ w_3' &= \frac{A_1}{3} w_2'^2 - \frac{2}{3} A_1 w_1 w_2', \\ w_4' &= w_5, \\ w_5' &= \frac{Pr\delta w_1 w_2 w_5 - \frac{2}{3} A_3 Pr w_1 w_5)}{\left(\left(A_2 + \frac{4}{3}Rd\right) - Pr\delta_1 x w_1^2\right)}, \end{aligned}\right\} \tag{22}$$

associated boundary conditions are

$$\left.\begin{aligned} &\eta = 0 : w_1(0) = 0, w_2(0) = 1 + \gamma_1\xi_1, w_4(0) = 1 + \gamma_2\xi_2, \\ &\eta \to \infty : w_2(\infty) \to 0, w_4(\infty) \to 0. \end{aligned}\right\} \tag{23}$$

In the situation of the present problem, the tolerance rate and convergence value were set at 10^{-6} and $\eta_\infty = 7$. Fig 3 is considered to illustrate the bvp4c numerical scheme's flow chart mechanism.

5. Verification of code

The comparative analyses of the findings achieved with those stated by Reddy et al. [27] with the variation in λ and γ by holding other parameters fixed are given in Table 2. To obtain numerical calculations, the Matlab software bvp4c method is utilized. It is fully known from Table 2 that the findings obtained are very reliable and accurate.

6. Discussion

This sector is dedicated to studying the effect of sundry parameters that appear during the numerical simulation of the problem against shear stress field, velocity field, temperature field. Table 3 is sketched for the analysis of various dimensionless parameters on shear stress fields

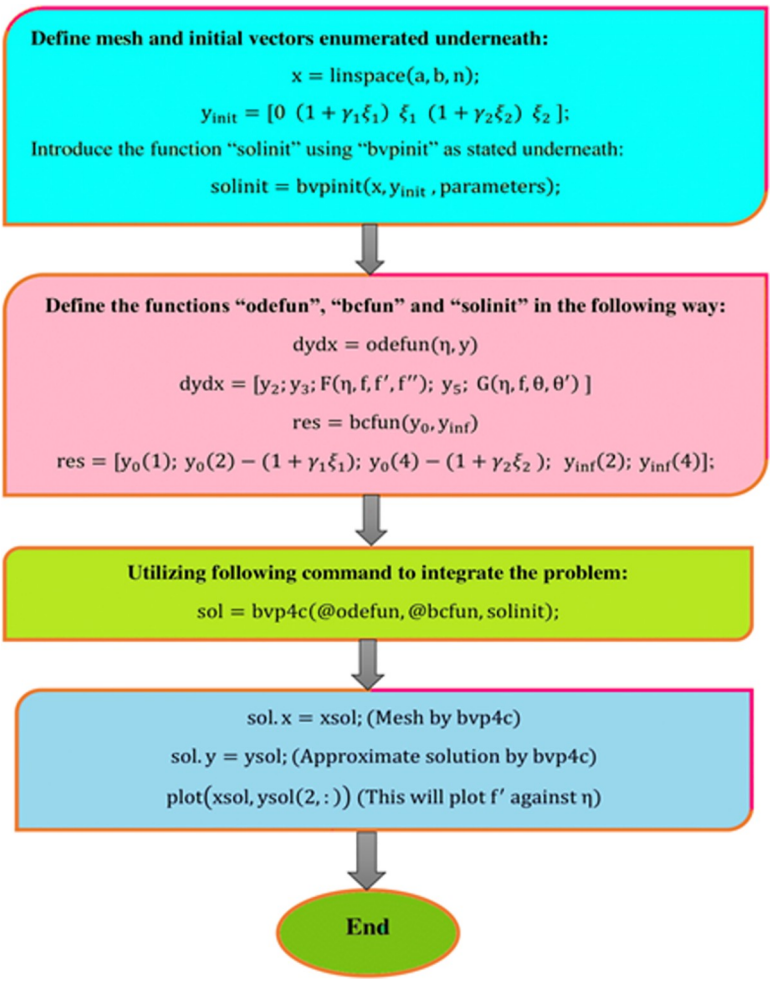

Fig 3. The bvp4c scheme's flow chart method.

https://doi.org/10.1371/journal.pone.0258367.g003

and the rate of heat transport for two kinds of CNTs. In the case of SWCNT, the domain of shear-stress $g(\eta)$ increases because of an increment in fluid factor λ but $g(\eta)$ lessens as a result of enrichment in Bingham number γ and velocity slip γ_1 but no alteration is detected for the case of radiation *Rd*, Prandtl number *Pr*, thermal relaxation time parameter δ, and temperature slip parameter γ_2. The rate of heat transport implies result in an improvement in λ, *Rd*, δ but heat transfer depreciates as a result of an improvement in the remaining parameters like γ, γ_1, γ_2, *Pr*. For the case of MWCNT, shear stress field $g(\eta)$ augments owing to amplification in λ but decreases in the case of γ and γ_1 and no change is obvious in the status of the remaining

Table 2. Study of the relation of present findings with Ref. [27] without *Rd*.

$Nu_x Re_x^{-1/2}$				
γ	$\lambda = 0.5$		$\lambda = 1.0$	
	Present	**Ref. [27]**	**Present**	**Ref. [27]**
0.1	0.130909	0.109782	0.144535	0.114058
0.2	0.109284	0.102621	0.144535	0.114058
0.3	0.085161	0.097438	0.144535	0.114058

https://doi.org/10.1371/journal.pone.0258367.t002

Table 3. Effect of distinct physical factors on the skin frictions and Nusselt number.

Physical parameters							SWCNT		MWCNT	
γ	λ	γ_1	Rd	Pr	δ	γ_2	$g(\eta)$	$Nu_x Re_x^{-1/2}$	$g(\eta)$	$Nu_x Re_x^{-1/2}$
0.5	0.1	0.1	0.1	24	0.01	0.1	0.3590	3.5454	0.3492	3.4368
0.7							0.2814	3.3449	0.2742	3.2533
0.9							0.2674	3.2413	0.2460	3.1585
1.1							0.2342	3.1713	0.2331	3.1099
	0.3						0.4734	3.6694	0.4629	3.5491
	0.5						0.5365	3.6983	0.5256	3.5752
	0.7						0.5821	3.7115	0.5709	3.5870
		0.3					0.3033	3.3963	0.2962	3.2991
		0.5					0.2661	3.2796	0.2605	3.1907
		0.7					0.2391	3.1843	0.2346	3.1018
			0.3				0.3590	3.3751	0.3492	3.2642
			0.5				0.3590	3.3931	0.3492	3.2812
			0.7				0.3590	3.4364	0.3492	3.3142
				25			0.3590	3.6227	0.3492	3.5104
				26			0.3590	3.6178	0.3492	3.5020
				27			0.3590	3.6009	0.3492	3.4816
					0.02		0.3590	3.5506	0.3492	3.4411
					0.03		0.3590	3.5557	0.3492	3.4453
					0.04		0.3590	3.5606	0.3492	3.4493
						0.3	0.3590	2.7954	0.3492	2.6880
						0.5	0.3590	2.3072	0.3492	2.2071
						0.7	0.3590	1.9642	0.3492	1.8721

https://doi.org/10.1371/journal.pone.0258367.t003

parameters. The number of Nusselt amplifies by the virtue of enrichment in the amounts of Rd, λ and δ. The Nusselt number depreciates as a result of an improvement in the remaining parameters like γ, γ_1, γ_2, Pr.

Tables 4 and 5 are designed to study the effect of thermal radiation and velocity slip condition on Nusselt number and skin friction coefficient. From Table 4, it is quite clear that the heat transfer rate increases by increasing the thermal radiation parameter and maximum value at $Rd = 2.5$ which is 18.5%. From Table 5, it is quite evident the skin friction coefficient depreciates as a result of amplification in the velocity slip parameter and the maximum decrement is 67.9%.

Fig 4 is designed to study the influence of RPF λ parameter on the profile of velocity $f'(\eta)$. It is observed at an improvement in λ, the fluid behaves like shear thinning and the fluid flows more freely on the surface of the sheet which amplifies the velocity of the fluid and velocity

Table 4. Heat transfer analysis in the presence/absence of thermal radiation.

Parameter	$Nu_x Re_x^{-1/2}$		$change = \left\lvert \frac{Presence - Absence}{Presence} \right\rvert \times 100\%$
Rd	Presence of Rd	Absence of Rd	
1	2.5099	2.2835	9.02%
1.5	2.6119	2.2835	12.6%
2	2.7094	2.2835	15.7%
2.5	2.8038	2.2835	18.5%

https://doi.org/10.1371/journal.pone.0258367.t004

Table 5. Velocity slip impact on the skin friction coefficient.

Parameter	$Cf_x Re_x^{1/2}$		$change = \left\| \frac{Presence - Absence}{Presence} \right\| \times 100\%$
γ_1	Presence of γ_1	Absence of γ_1	
0.1	0.6284	0.6938	10.4%
0.3	0.5322	0.6938	30.3%
0.5	0.4642	0.6938	49.5%
0.7	0.4130	0.6938	67.9%

https://doi.org/10.1371/journal.pone.0258367.t005

profile. The Bingham number γ effect on the domain of velocity is represented in Fig 5. The proportion of yield-stress to viscous-stress is the number of Bingham. It is noted that due to an increase in the shear-rate, the fluid viscosity increases. Physically, amplification in Bingham turns liquid into solids due to magnification in the fluid viscosity. The fluid then behaves like shear-thickening, which often diminishes the velocity of the fluid. Fig 6 revealed the effect of velocity slip γ_1 on $f'(\eta)$. Slip phenomenon occurs when the velocity of the nanofluid and the surface is not the same. Physically, the slip phenomenon occurs due to roughness, wetness, and non-adhesives forces acting on the surface of the stretching sheet. That's why they wander wall forces and adhesives forces are not acting on the fluid flow over the stretching sheet. As a result slip phenomenon occurs. In the presence of slip phenomenon, the nanofluid velocity flow over the surface declines which lessens the fluid velocity and $f'(\eta)$. The portrayal of γ on shear stress field $g(\eta)$ is shown in Fig 7. It's noted that the shear stress field diminishes owing to amplification in γ. Physically for the fewer values of γ and λ, the fluid behaviour is shear thickening. Both γ and λ are prominent factors of the Reiner-Philippoff fluid parameter and are somehow related to each other. The behaviour of the fluid is shear-thinning $\lambda<1$ which lessens the fluid velocity and amplifies the stress field. As a result $g(\eta)$ augments. Fig 8 depicts the outcome of λ on $g(\eta)$. Fluid parameter λ is the ratio of zero shear rate to the infinite sheat rate. Physically a positive variation in the infinite shear rate depreciates the fluid parameter λ.

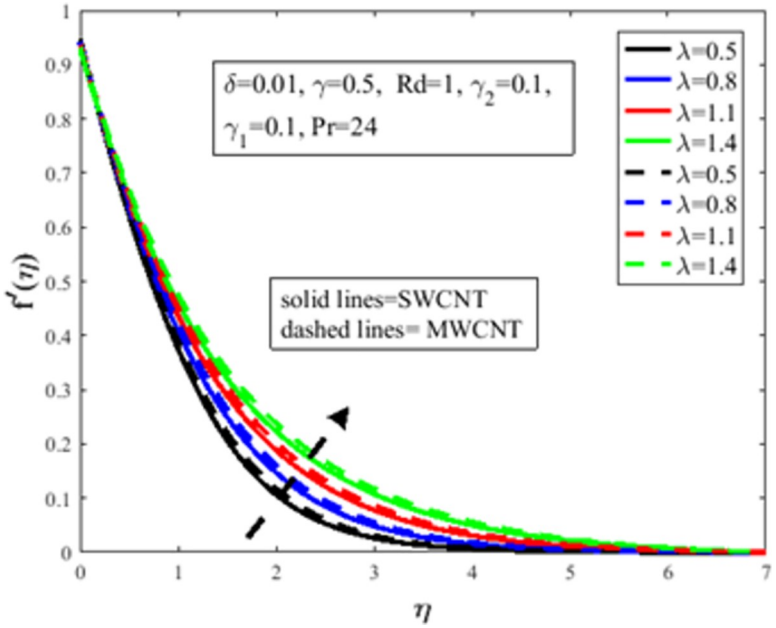

Fig 4. Effect of λ on $f'(\eta)$.

https://doi.org/10.1371/journal.pone.0258367.g004

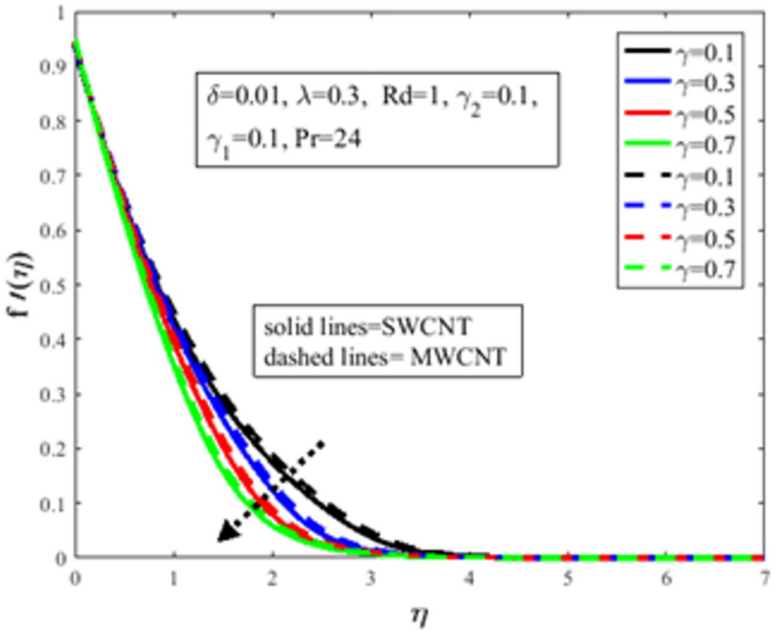

Fig 5. Effect of γ on $f'(\eta)$.

https://doi.org/10.1371/journal.pone.0258367.g005

The viscosity of fluid abates by the virtue of an amplification in λ which lessens the shear-stress of the nanofluid that furthermore leads to a decrement in the domain of shear-stress. Fig 9 is designed to reflect the effect of nanoparticles concentration ϕ on the profile of velocity. Physically concentration is proportional to the diffusivity. Molecules diffuse more quickly by the virtue of an increment in the concentration of nanoparticles. Concentration of the fluid increases

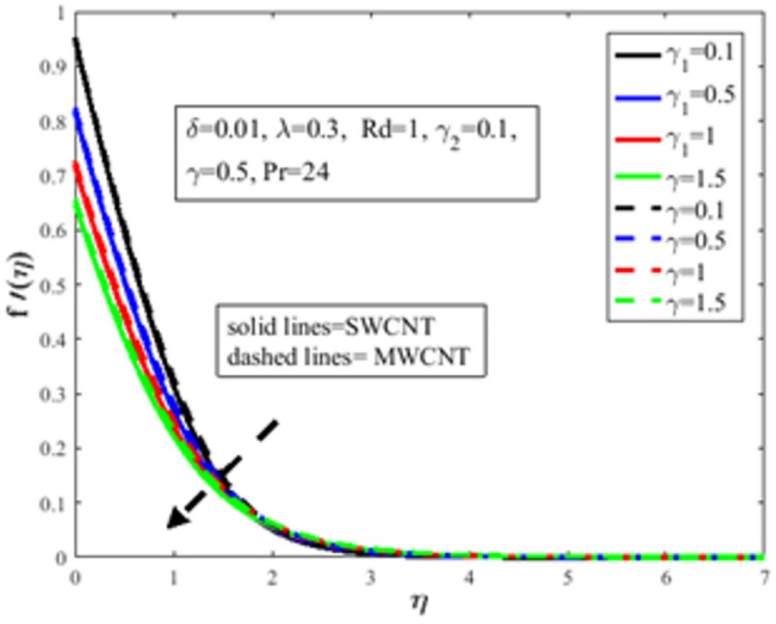

Fig 6. Effect of γ_1 on $f'(\eta)$.

https://doi.org/10.1371/journal.pone.0258367.g006

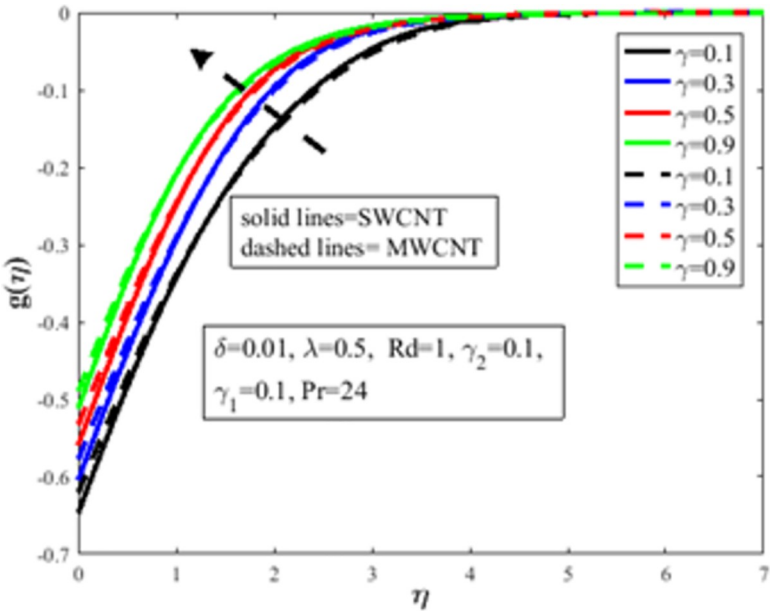

Fig 7. Effect of γ on $g(\eta)$.

https://doi.org/10.1371/journal.pone.0258367.g007

due to an augmentation in the nanoparticles concentration of nanoparticles which lessens the fluid flow that eventually diminishes the velocity of nanofluid.

In Fig 10, the Prandtl number Pr impact on the distribution of temperature field $\theta(\eta)$ is illustrated. The number of Prandtl is the proportion of momentum diffusion and thermal diffusion. Physically Pr is one of the prominent factors of boundary layer analysis. In the case of $Pr<1$, the thermal boundary layer dominates the momentum boundary layer but the situation is quite opposite in the case of $Pr>1$ where the momentum boundary layer dominates the

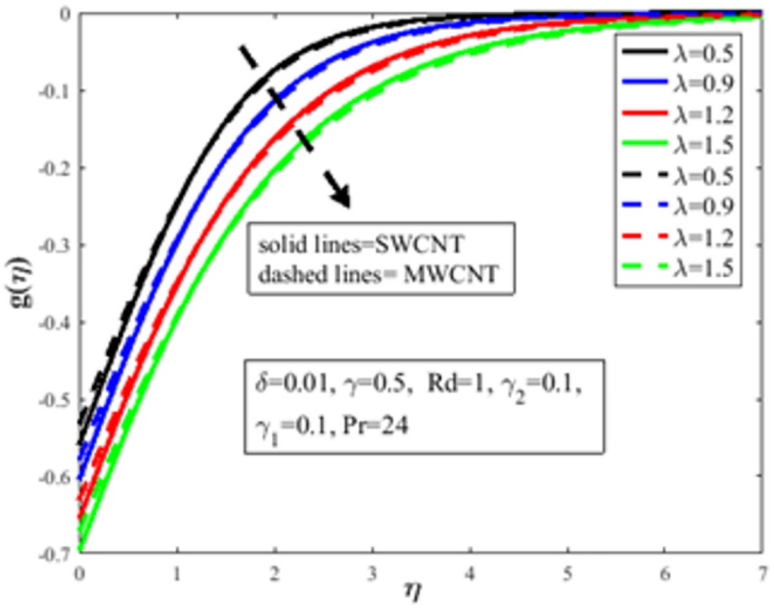

Fig 8. Effect of λ on $g(\eta)$.

https://doi.org/10.1371/journal.pone.0258367.g008

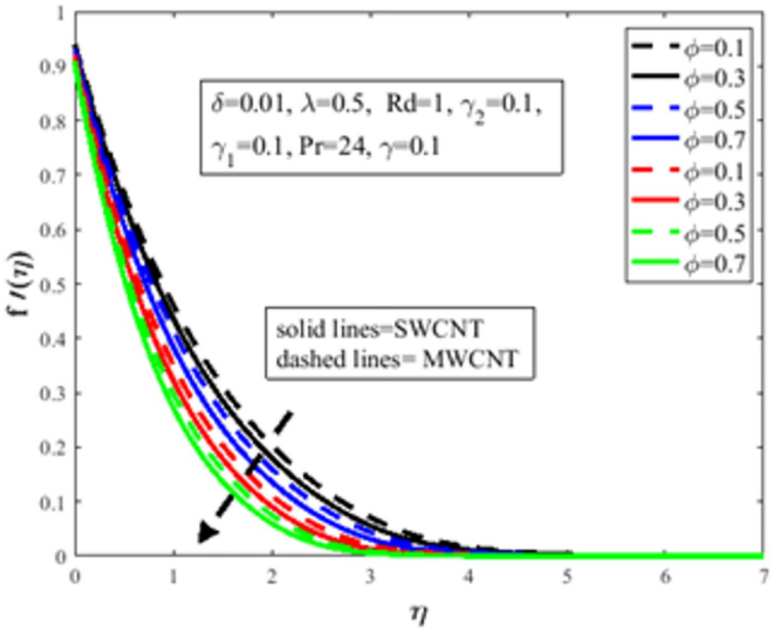

Fig 9. Effect of ϕ on $g(\eta)$.

https://doi.org/10.1371/journal.pone.0258367.g009

thermal boundary layer. It is well established, the thermal diffusion of the fluid diminishes result in an increase in *Pr*. The temperature of the fluid depreciates as a result of an abatement in the thermal diffusivity which furthermore guides to a decrement in $\theta(\eta)$. The characteristics of radiation parameter *Rd* on $\theta(\eta)$ are highlighted in Fig 11. Physically thermal radiation is used to enhance the heat transfer rate of the fluid having immense utilization in an industry like polymer production, combustion reactors, pasteurization, and remove toxic

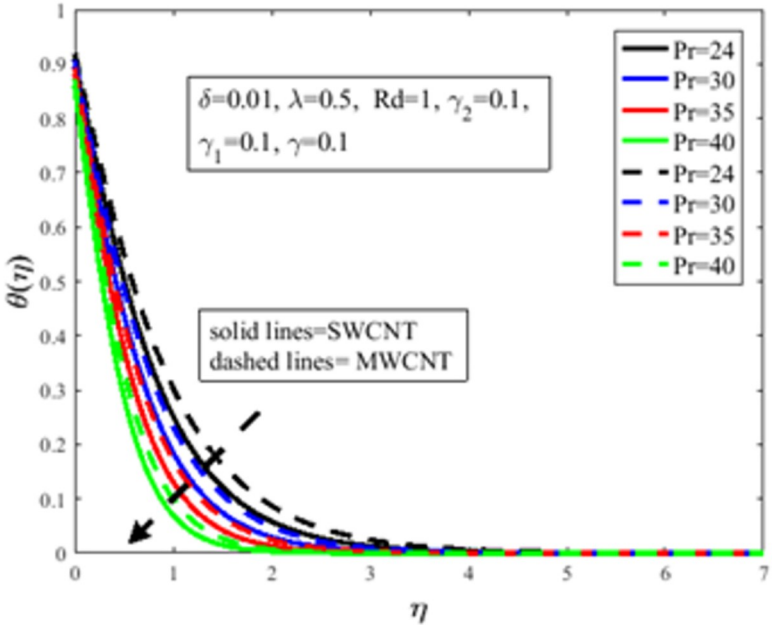

Fig 10. Effect of *Pr* on $\theta(\eta)$.

https://doi.org/10.1371/journal.pone.0258367.g010

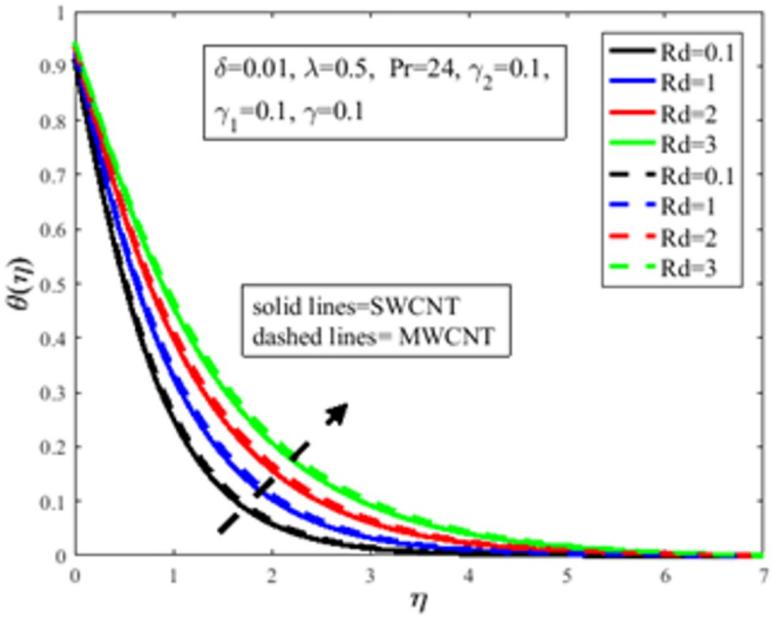

Fig 11. Effect of *Rd* on $\theta(\eta)$.

https://doi.org/10.1371/journal.pone.0258367.g011

microorganisms from the liquids. Sun is the best source of thermal radiation. Radiations enhance the nanofluid temperature. In the presence of *Rd* heat enter more easily into the system which improves the fluid temperature and temperature field $\theta(\eta)$. Fig 12 elucidates the influence of the temperature slip factor γ_2 on the temperature profile $\theta(\eta)$. Physically temperature slip phenomenon occurs when the temperature of the sheet and fluid flow over the sheet is not in thermal equilibrium. With temperature slip condition, the temperature of the

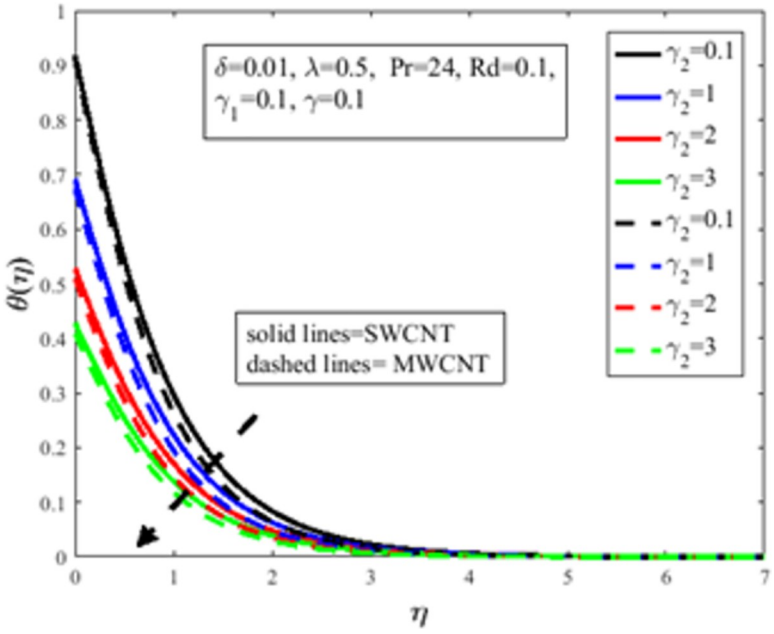

Fig 12. Effect of γ_2 on $\theta(\eta)$.

https://doi.org/10.1371/journal.pone.0258367.g012

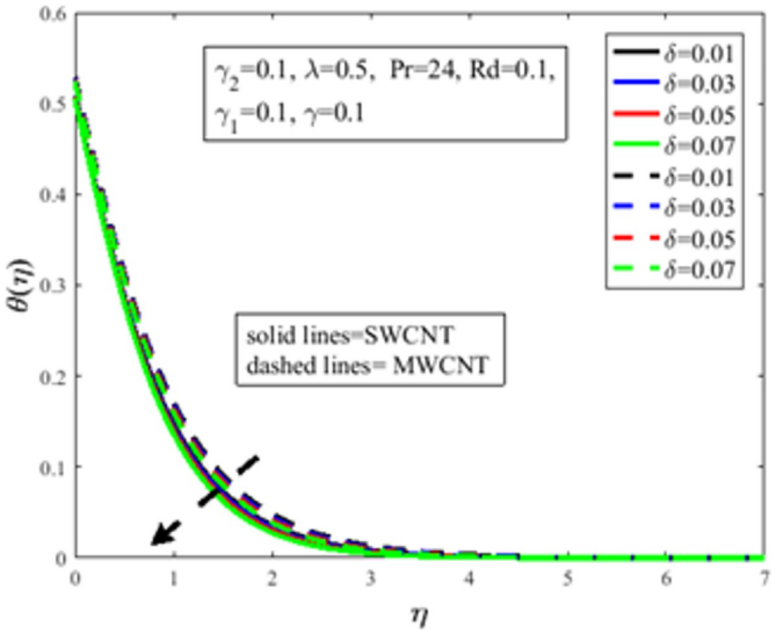

Fig 13. Effect of δ on $\theta(\eta)$.

https://doi.org/10.1371/journal.pone.0258367.g013

nanofluid declines which lessens the fluid temperature and $\theta(\eta)$. Fig 13 exhibits the parameter dependencies of thermal relaxation δ on the temperature field $\theta(\eta)$. Physically thermal relaxation time is the time in which fluid is allowed to relax to retain its original shape. During this time the fluid behaviour is shear thickening. As a result of a rise in δ, the nanofluid particles show nonconducting behaviour, which takes a long time to convey heat to their neighboring nearby particles. The temperature distribution diminishes as a consequence. Fig 14 illustrates

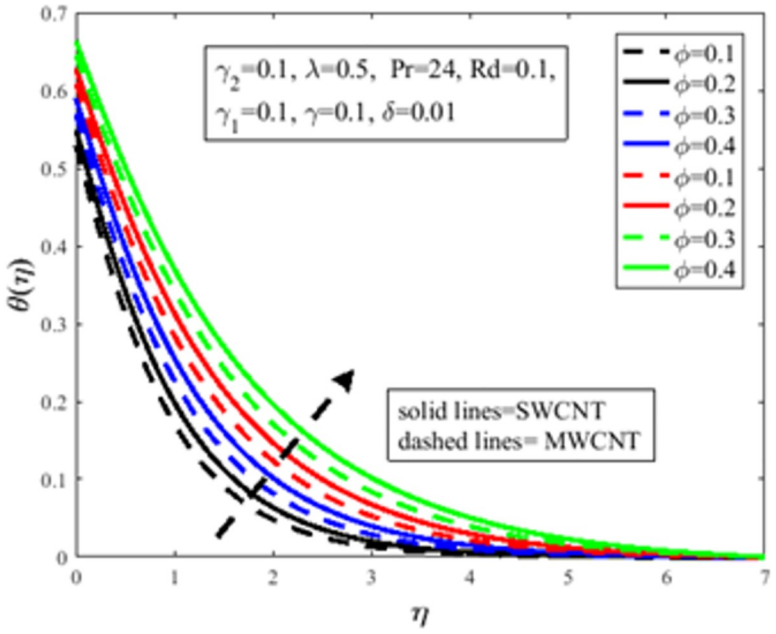

Fig 14. Effect of ϕ on $\theta(\eta)$.

https://doi.org/10.1371/journal.pone.0258367.g014

the influence of nanoparticles concentration ϕ on $\theta(\eta)$. Physically it is quite evident that the insertion of nanoparticles in the base fluid enhances the thermal conductivity of the fluid and ultimately amplifies the heat transfer rate. The thermal conductivity of nanoparticles increases owing to an amplification in ϕ which moreover augments the temperature of fluid and $\theta(\eta)$.

7. Conclusion

In the present research, a computational heat transfer of Reiner-Phillipoff nanofluids over a flat surface is investigated under the impact of Maxwell velocity slip and Smoluchowski temperature slip on CNTs with modified Fourier theory. The concluding remarks from this study are given below

- An improvement in the fluid parameter λ escalates the velocity field but the fluid velocity depreciates by the virtue of amplification in the Bingham number γ.
- The shear-stress domain depressed results in enrichment in the fluid factor λ.
- Velocity of the fluid lessens due to an increment in the concentration of nanoparticles.
- An amplification in velocity slip γ_1 and temperature slip γ_2 depreciates velocity and temperature profiles.
- A positive variation in a parameter of thermal relaxation δ brings about a decrement in the temperature distribution.
- Temperature field escalates by the virtue of amplification in the radiation parameter *Rd*.
- Rate of heat transport augments owing to an augmentation in the volume fraction of nanoparticles.

Supporting information

S1 Nomenclature.
(DOCX)

Author Contributions

Conceptualization: Tanveer Sajid, Mohamed R. Eid, Kottakkaran Sooppy Nisar.

Data curation: Tanveer Sajid, Faisal Shahzad, Mohamed R. Eid, Kottakkaran Sooppy Nisar.

Formal analysis: Tanveer Sajid, Wasim Jamshed, Faisal Shahzad, Mohamed R. Eid, Kottakkaran Sooppy Nisar.

Funding acquisition: M. A. Aiyashi, Kottakkaran Sooppy Nisar, Anurag Shukla.

Investigation: Wasim Jamshed.

Methodology: Wasim Jamshed, Mohamed R. Eid.

Project administration: Mohamed R. Eid.

Resources: Tanveer Sajid, Wasim Jamshed, Mohamed R. Eid, Kottakkaran Sooppy Nisar.

Software: Wasim Jamshed, Faisal Shahzad, Mohamed R. Eid, Kottakkaran Sooppy Nisar.

Supervision: Wasim Jamshed, Mohamed R. Eid, Kottakkaran Sooppy Nisar.

Validation: Tanveer Sajid, Wasim Jamshed, Mohamed R. Eid, Kottakkaran Sooppy Nisar.

Visualization: Wasim Jamshed, Faisal Shahzad, M. A. Aiyashi, Mohamed R. Eid, Anurag Shukla.

Writing – original draft: Tanveer Sajid, Wasim Jamshed, Faisal Shahzad, Mohamed R. Eid, Kottakkaran Sooppy Nisar.

Writing – review & editing: Tanveer Sajid, Wasim Jamshed, Faisal Shahzad, M. A. Aiyashi, Mohamed R. Eid, Anurag Shukla.

References

1. EKundu P. K., Chakraborty T., Das K., Framing the Cattaneo-Christov heat flux phenomena on CNT-based Maxwell nanofluid along stretching sheet with multiple slips, *Arabian Journal for Science and Engineering* 43(3) (2018) 1177–1188.
2. Al-Hanaya A. M., Sajid F., Abbas N., Nadeem S., Effect of SWCNT and MWCNT on the flow of micropolar hybrid nanofluid over a curved stretching surface with induced magnetic field, *Scientific Reports* 10 (1) (2020) 1–18. https://doi.org/10.1038/s41598-019-56847-4 PMID: 31913322
3. Hayat T., Hussain Z., Alsaedi A., Hobiny A., Computational analysis for velocity slip and diffusion species with carbon nanotubes, *Results in Physics* 7 (2017) 3049–3058.
4. Nagalakshm P.S.S., Vijaya N., MHD flow of Carreau nanofluid explored using CNT over a nonlinear stretched sheet, *Frontiers in Heat and Mass Transfer* 14 (2020) 1–9.
5. Muhammad S., Ali G., Shah Z., Islam S., Hussain S. A., The rotating flow of magneto hydrodynamic carbon nanotubes over a stretching sheet with the impact of non-linear thermal radiation and heat generation/absorption, *Applied Sciences* 8(4) (2018) 482.
6. Khalid A., Khan I., Khan A., Shafie S., Tlili I., Case study of MHD blood flow in a porous medium with CNTS and thermal analysis, *Case Studies in Thermal Engineering* 12 (2018) 374–380.
7. Hosseinzadeh Kh., Roghani So., Mogharrebi A.R., Asadi A., Waqas M., Ganji D.D., Investigation of cross-fluid flow containing motile gyrotactic microorganisms and nanoparticles over a three-dimensional cylinder, *Alexandria Engineering Journal*, 59 (2020) 3297–3307.
8. Mogharrebi A.R., Ganji A.R.D., Hosseinzadeh K., Roghani S., Asadi A., Fazlollahtabar A., Investigation of magnetohydrodynamic nanofluid flow contain motile oxytactic microorganisms over rotating cone, *International Journal of Numerical Methods for Heat & Fluid Flow* (2021). https://doi.org/10.1108/HFF-08-2020-0493
9. Lu D., Ramzan M., Mohammad M., Howari F., Chung J. D., A thin film flow of nanofluid comprising carbon nanotubes influenced by Cattaneo-Christov heat flux and entropy generation, *Coatings* 9(5) (2019) 296.
10. Mandal P. K., Seth G. S., Sarkar S., Chamkha A., A numerical simulation of mixed convective and arbitrarily oblique radiative stagnation point slip flow of a CNT-water MHD nanofluid, *Journal of Thermal Analysis and Calorimetry* (2020) 1–16. https://doi.org/10.1007/s10973-020-10344-3
11. Chaudhary S., Kanika K. M., Galerkin finite-element numerical analysis of the effects of heat generation and thermal radiation on MHD SWCNT-water nanofluid flow with a stretchable plate, *Pramana* 94(1) (2020) 38.
12. Gholinia M., Hosseinzadeh Kh., Ganji D. D., Investigation of different base fluids suspend by CNTs hybrid nanoparticle over a vertical circular cylinder with sinusoidal radius, *Case Studies in Thermal Engineering* 21 (2020) 100666.
13. Hosseinzadeh K., Mardani M., Salehi S., Paikar M., Waqas M., Ganji D., Entropy generation of three-dimensional Bödewadt flow of water and hexanol base fluid suspended by Fe_3O_4 and MoS_2 hybrid nanoparticles, *Pramana* 95(2) (2021) 1–14.
14. Hosseinzadeh K., Montazer E., Shafii M. B., Ganji D., Heat transfer hybrid nanofluid (1-Butanol/MoS_2–Fe_3O_4) through a wavy porous cavity and its optimization, *International Journal of Numerical Methods for Heat & Fluid Flow* 31 (2020) 1547–1567.
15. Salehi S., Nori A., Hosseinzadeh K., Ganji D., Hydrothermal analysis of MHD squeezing mixture fluid suspended by hybrid nanoparticles between two parallel plates, *Case Studies in Thermal Engineering* 21 (2020) 100650.
16. Cattaneo C., Sulla conduzione Del Calore, *Atti del Seminario Matematico e Fisico dell Universita di Modena e Reggio Emilia* pages 3 (1948) 83–101.
17. Christov C. I., On frame indifferent formulation of the Maxwell-Cattaneo model of finite speed heat conduction, *Mechanics Research Communications* 36 (2009) 481–486.

18. Akbar N. S., Khalique C. M., Khan Z. H., Cattaneo-Christov heat flux model study for water-based CNT suspended nanofluid past a stretching surface, *Nanofluid heat and mass transfer in engineering problems*, IntechOpen (2017).

19. Ali U., Alqahtani A. S., Rehman K. R., Malik M. Y., On Cattaneo-Christov heat flux analysis with magneto-hydrodynamic and heat generation effects in a Carreau nano-fluid over a stretching sheet, *Revista Mexicana De Fisica* 65(5) (2019) 479–488.

20. Ibrahim W., Sisay G., Gamachu D., Mixed convection flow of Oldroyd-B nano fluid with Cattaneo-Christov heat and mass flux model with third order slip, *AIP Advances* 9(12) (2019) 125023.

21. Rasool G., Zhang T., Darcy-Forchheimer nanofluidic flow manifested with Cattaneo-Christov theory of heat and mass flux over non-linearly stretching surface, *PLoS One* 14(8) (2019) e0221302. https://doi.org/10.1371/journal.pone.0221302 PMID: 31430309

22. Khan U., Ahmad S., Hayyat A., Khan I., Nisar K. S., Baleanu D., On the Cattaneo-Christov heat flux model and OHAM analysis for three different types of nanofluids, *Applied Sciences* 10(3) (2020) 886.

23. Shah Z., Tassaddiq A., Islam S., Alklaibi A. M., Khan I., Cattaneo-Christov heat flux model for three-dimensional rotating flow of SWCNT and MWCNT nanofluid with Darcy-Forchheimer porous medium induced by a linearly stretchable surface, *Symmetry* 11(3) (2019) 331.

24. Dogonchi A. S., Ganji D. D., Impact of Cattaneo-Christov heat flux on MHD nanofluid flow and heat transfer between parallel plates considering thermal radiation effect, *Journal of the Taiwan Institute of Chemical Engineers* 80 (2017) 52–63.

25. Sreedevi P., Reddy P. S. Heat and mass transfer analysis of MWCNT kerosene nanofluid flow over a wedge with thermal radiation, *Heat Transfer* (2020) 1–24. https://doi.org/10.1002/htj.21892

26. Shah Z., Dawar A., Kumam P., Khan W., Islam S. Impact of nonlinear thermal radiation on MHD nanofluid thin film flow over a horizontally rotating disk, *Applied Sciences* 9(8) (2019) 1533.

27. Reddy M. G., Sudharani M. V. V. N. L., Kumar K. G., Chamkha A. J., Lorenzini G. Physical aspects of Darcy-Forchheimer flow and dissipative heat transfer of Reiner-Philippof fuid, *Journal of Thermal Analysis and Calorimetry* 141 (2020) 829–838.

28. Khan N. S., Gul T., Islam S., Khan W. Thermophoresis and thermal radiation with heat and mass transfer in a magnetohydrodynamic thin-film second-grade fluid of variable properties past a stretching sheet, *The European Physical Journal Plus* 132(1) (2017) 11.

29. Hosseinzadeh Kh., Asadi A., Mogharrebi A. R., Azari M. E., Ganji D. D., Investigation of mixture fluid suspended by hybrid nanoparticles over vertical cylinder by considering shape factor effect, *Journal of Thermal Analysis and Calorim*etry 143 (2021) 1081–1095.

30. Kumar K. G., Rudraswamy N. G., Gireesha B. J., Krishnamurthy M. R., Influence of nonlinear thermal radiation and viscous dissipation on three-dimensional flow of Jeffrey nano fluid over a stretching sheet in the presence of Joule heating, *Nonlinear Engineering* 6(3) (2017) 207–219.

31. Makinde O. D., Kumar K. G., Manjunatha S., Gireesha B. J., Effect of nonlinear thermal radiation on MHD boundary layer flow and melting heat transfer of micro-polar fluid over a stretching surface with fluid particles suspension, *Defect and Diffusion Forum* 378 (2017) 125–136.

32. Ahmed N., Adnan U. Khan, S. T. Mohyud-Din, Influence of thermal radiation and viscous dissipation on squeezed flow of water between riga plates saturated with carbon nanotubes, *Colloids and Surfaces A*: *Physicochemical and Engineering Aspects* 522 (2017) 389–398.

33. Hosseinzadeh Kh., Salehi S., Mardani M. R., Mahmoudi F. Y., Waqas M., Ganji D. D., Investigation of nano-Bioconvective fluid motile microorganism and nanoparticle flow by considering MHD and thermal *radiation*, Informatics in Medicine Unlocked 21 (2020) 100462.

34. Hosseinzadeh Kh., Roghani S., Mogharrebi A. R., Asadi A., Ganji D.D., Optimization of hybrid nanoparticles with mixture fluid flow in an octagonal porous medium by effect of radiation and magnetic field. *Journal of Thermal Analysis and Calorimetry* 143 (2021) 1413–1424.

35. Rashed G., El-Fayez F., Thermal radiation and thermal diffusion for Soret and Dufour's effects on MHD flow over rotating infinite disk, *Nanofluid Flow in Porous Media*. IntechOpen, (2019).

36. Shafiq A., Rasool G., Khalique C. M., Significance of thermal slip and convective boundary conditions in three dimensional rotating Darcy-Forchheimer nanofluid flow, *Symmetry* 12(5) (2020) 741.

37. Mukhopadhyay S., Effects of slip on unsteady mixed convective flow and heat transfer past a stretching surface, *Chinese Physics Letters* 27(12) (2010) 124401.

38. Raza J., Thermal radiation and slip effects on magnetohydrodynamic (mhd) stagnation point flow of Casson fluid over a convective stretching sheet, *Propulsion and Power Research* 8(2) (2019) 138–146.

39. Abbas N., Malik M. Y., and Nadeem S. Stagnation flow of hybrid nanoparticles with MHD and slip effects. *Heat Transfer-Asian Research*, 49(1):180–196, 2020.

40. Rao A. S., Prasad V. R., Radhika V. N., Beg O. A. Heat transfer in viscoplastic boundary-layer flow from a vertical permeable cone with momentum and thermal wall slip: numerical study, *Heat Transfer Research* 49(3) (2018) 189–204.

41. Sejunti M. I., Khaleque T. S., Effects of velocity and thermal slip conditions with radiation on heat transfer flow of ferrofluids, *Journal of Applied Mathematics and Physics* 7(6) (2019) 1369–1387.

42. Li C. Y., Keh H. J., Thermophoresis of a particle in a concentric cavity with thermal stress slip, *Aerosol Science and Technology* 52(3) (2018) 269–276.

43. Sarabandi A. H., Moghadam J. A., Slip velocity in flow and heat transfer of non-newtonian fluids in microchannels, *International Journal of Engineering* 30(7) (2017) 1054–1065.